HEFAT2011
8th International Conference on Heat Transfer, Fluid Mechanics and Thermodynamics
11 – 13 July 2011
Pointe Aux Piments, Mauritius

MORPHOLOGICAL INSTABILITY OF THE SEA ICE – OCEAN INTERFACE IN THE PRESENCE OF BRINE CHANNELS IN A MUSHY LAYER

Alexandrov D.V.* and Malygin A.P.
*Author for correspondence
Department of Mathematical Physics,
Urals State University,
Ekaterinburg, 620083,
Russian Federation,
E-mail: dmitri.alexandrov@usu.ru

ABSTRACT

The formation of brine channels during the solidification process has a significant impact on the structure of the two-phase zone (mushy layer). They are responsible for the formation of another crystallization scenario and the generation of corrugations of the sea ice–ocean interface. The physical mechanism relies on brine flows developing in the sea ice due to Bernoulli suction by flow of ocean past the liquid–mushy layer interface. This mechanism should be particularly very important during sea ice freezing in wind-maintained coastal polynyas and in leads changing thermal fluxes and the heat and mass balance of the Arctic sea ice cover. Generally speaking, a true criterion of the formation of such a regime is connected with the morphological stability analysis of the mushy layer crystallization with respect to small perturbations of its morphology. In the present paper, we develop the morphological stability analysis of the directional crystallization with brine channels in a two-phase region and give a new stability criterion taking into account perturbations in the impurity concentration (salinity) and solid fraction distributions for the case of nonturbulent and turbulent boundary conditions at the mush–ocean interface.

INTRODUCTION

Directional solidification of melts and liquids underlies many technologies employed in traditional and new industries (metallurgy, crystal growth, energetics, chemistry, aerospace engineering, electronics) and describes natural processes (formation of ices, crystallization of lava-streams, crystal growth in supersaturated solutions). In spite of the extended history of study of solidification, many aspects of the physics of this phenomenon remain unclear. Aspects of forming of various types of micro- and macrostructures in solids and liquids, the physical mechanisms of which remain to a large degree unclear, are of particular importance. Traditionally the study of solidification was and is performed within the framework of the classical model, leading to the Stefan-type boundary value problem [1,2]. In this approach it is assumed that the liquid and solid phases are separated by a clearly expressed smooth interface between the phases, heat transfer occurs by conduction according to the Fourier law and the velocity of the crystallization front is controlled by the absorption of heat by the solid phase. The mathematical formulations corresponding to these physical models belong to the class of highly-nonlinear problems with moving boundaries. In spite of the appreciable progress attained in investigating these problems, it became clear during the past several years that this approach is limited. This is because the developments of experimental data on materials with specified properties necessitate investigating a number of new dynamic phenomena typical of the solidification process. These phenomena include the formation of cellular and dendritic structures and the formation of transition mushy regions that separate the crystal and the liquid.

NOMENCLATURE

c	[J/kgK]	Specific heat capacity
C	[psu]	Salinity
D	[m^2/s]	Diffusion coefficient
$\vec{g}$	[m/s^2]	Acceleration due to gravity
G	[K/m]	Linear temperature gradient in the mushy layer
i	[-]	Imaginary unit
k	[J/mKs]	Thermal conductivity coefficient
k_0	[-]	Equilibrium partition coefficient
L	[J/kg]	Latent heat released per unit mass
m	[K/psu]	Liquidus slope
$\vec{n}$	[-]	Unit normal at the interface pointing into the ocean
p_1	[kg/ms^2]	Pressure
t	[s]	Time
T	[K]	Temperature
T_*	[K]	Phase transition temperature of the pure mixture
$\vec{u}$	[m/s]	'Darcy' velocity, which is the volume flux of brine per unit perpendicular, cross-sectional area flowing between the ice crystals
u_*	[m/s]	Friction velocity

U	[m/s]	Velocity of a uniform flow in the ocean parallel to the undisturbed interface
V	[m/s]	Normal growth velocity of the mushy layer - ocean interface
x	[m]	Spatial coordinate directed along the mushy layer – ocean interface
z	[m]	Spatial coordinate directed from the mushy layer to the ocean

Special characters

α	[1/m]	Wave number of the perturbation
α_h	[-]	Turbulent coefficient for heat
α_s	[-]	Turbulent coefficient for salt
β	[-]	Coefficient of permeability (anisotropy)
γ	[1/m]	Coefficient of inhomogeneity (heterogeneity)
$\hat{\zeta}$	[m]	Perturbation amplitude of the mushy layer – ocean interface
$\hat{\theta}$	[K]	Perturbation amplitude of the temperature field
μ	[kg/ms]	Dynamic viscosity
ν	[m^2/s]	Kinematic viscosity
ρ	[kg/m^3]	Density
σ	[1/s]	Growth rate of perturbations
φ	[-]	Solid fraction in the mushy layer
φ_0	[-]	Unperturbed solid fraction in the mushy layer
Π	[m^2]	Permeability
Π_h	[m^2]	Permeability to horizontal flows
Π_v	[m^2]	Permeability to vertical flows
Φ	[m^2/s]	Velocity potential
$\hat{\Phi}$	[-]	Perturbation amplitude of the solid fraction

Subscripts

b	Designates the physical parameters on the mushy layer – ocean interface
l	Designates the physical parameters in the liquid phase
m	Designates the physical parameters in the mushy layer
s	Designates the physical parameters in the solid phase
∞	Designates the physical parameters in the ocean far from the mushy layer

In addition, it has been currently recognized that in order to explain the real structure of solid materials it is necessary to take account of the actual supercooling (undercooling) of the liquid and the consequence of appearance of metastability. Analysis of available data allows singling out several fundamental theoretical and applied problems. Firstly, the colossal complexity of the physical problems that arise when making allowance for phase transitions requires developing radically new approach to constructing models of solidification, which would include various kinds of nonlinear phenomena. An important role among these are nucleation, kinetics, fluid flows, convection and evolution of a new phase in a metastable medium, which in themselves require refining established and developing new approaches. Secondly, this gives rise to the need of mathematical formulation of the corresponding mathematical models, which requires establishing new classes of crystallization problems and developing methods for investigating them.

A number of important contributions to the study of these problems has been made previously. Ivantsov [3] demonstrated that, under certain conditions, a region of impurity - induced supercooling i.e., one in which the temperature is lower than the temperature of the phase transition, forms in the melt. Subsequent to this, a relationship between this phenomenon and the structure of the solid and liquid phases was rather rapidly recognized, which has brought about intensive studies of the crystallization dynamics. Mathematical models of crystallization are complicated by the need to apply boundary conditions at solid/liquid interfaces which are evolving with time and whose positions must be found as part of the calculation. The case of a pure melt being cooled by conduction of heat to its boundaries is relatively straightforward since the geometry of the solidification front is similar to that of the bounding walls [4]. However, if a pure melt is supercooled (has a temperature below its freezing point), so that latent heat is conducted away from the solidification front through the liquid, then the solidification front becomes extremely convoluted and forms intricate branching patterns [5]. Snowflakes provide a common example of this phenomenon. When the liquid is an alloy (a mixture of two or more components) such behavior is commonplace even when the liquid is not initially supercooled. At present, analytical techniques cannot follow the evolution of such convolutions far beyond initial perturbations from a flat interface. However, for many applications including metallurgy [6], solidification in magma chambers [7], and the structure of the Earth's inner core [8,9], it is the gross features of the solid-liquid matrix which forms as a result of the convolutions. The matrix or region of mixed phase is termed a "mush" or "mushy layer". By treating the mush as a new single phase, and the macroscopic envelope of the convoluted solid as a phase boundary, it is necessary to follow the evolution of two-phase boundaries: the solid/mush interface and the mush/liquid interface. Hills, Loper and Roberts [10] develop a full set of thermodynamic equations for a mushy zone, and solved a mushy-reduced set of them approximately for the constrained growth of a binary alloy. Also, these model equations were solved approximately by Fowler [11]. Hereafter, a fuller analyses and exact analytical solutions of them were suggested by Alexandrov [12-14]. More general sets of nonstationary equations and their self-similar solutions have been proposed by Worster [15] based upon simple considerations of local heat and mass balances. After, this model has been developed for the description of convective flows in the mushy layer in the absence of solute diffusion in the mush [16,17]. This phenomenon leads to the formation of chimneys (channels), which are narrow, dendrite-free regions that form within the mushy layer as a result of convection. This striking phenomenon is known to occur within solidifying alloys [18], where it is responsible for undesirable material properties; within sea-ice [19], where it has a significant effect on ocean dynamics; within magma chambers [20], where it influences mineral deposits, and it may occur at the Earth's inner-outer corner boundary [21,22]. When the convection is sufficiently strong, the solute-rich material that flows out of the mushy layer locally depresses the melting temperature, redissolving some of the dendrites. In this paper, we develop a mathematical model and give its stability analysis for the mushy layer filled with chimneys. By virtue of the fact that many laboratory and field observations are connected with the evolution of saltwater, let us give a short summary on the phase evolution of sea ices.

Recent studies of the ice cover changes have refocused attention on the correct description of local processes that have large scale consequences. For instance, the growth and decay of sea ice in the polar regions is the high-latitude equivalent of the

evaporation-precipitation cycle in the remainder of the world's oceans [23]. The evolution of brine channels in the sea ice mushy layer is responsible for the global climate consequences. Since the seasonal difference in sea ice coverage is $8 \cdot 10^6$ km^2 in the Arctic and $18 \cdot 10^6$ km^2 in the Antarctic, the dynamics of the brine rejection processes has a substantial impact on the stability of the oceanic mixed layer and the flux of fresh water into the North Atlantic Ocean, indicating that sea ice export is an important control in convective stability [24]. Another example is connected with cracks in the perennial ice cover, known as leads. Field observations in the Arctic show that the heat loss through these cracks can be up to 300 Wm^{-2}, or fifteen times that from the surrounding ice [25]. Although leads occupy less than 10% of the surface area, they are responsible for roughly half of the total oceanic heat loss. It is known that sea ice growth can be sufficiently fast. Its depth in 8-10 cm can be attained in the first twenty-four hours [26,27]. A rapid growth of such young sea ice produces the greatest heat flux, so the role of brine drainage on the phase evolution is significant in determining the overall heat budget.

When a binary liquid mixture (sea water) is cooled and solidified from above, the process can be described within the framework of the Stefan model with a planar front for as long as the impurity concentration gradient at the front is less than the temperature one [3,15]. Once this inequality has been broken up by the impurity displacement, the solid growing from such a liquid mixture usually forms a porous two-phase layer (mushy layer) in which concentrated liquid surrounds nearly pure solid matrix [28]. The dense, enriched liquid can be trapped within the matrix if it has insufficient negative buoyancy to overcome dynamically the resistance provided by the solid phase. Laboratory experiments [29] show that the composition remains essentially constant in the liquid region in the early stages of the mushy layer solidification. In other words, there is little transport of salt out of the mushy layer. Once the mushy layer has reached a critical thickness h_C, the concentration of salt in the liquid region suddenly begins to increase (see, for example, figures in refs. [29,30]). This increase is associated with the appearance of convective plumes, which emanate from channels within the mushy layer.The brine draining through channels in the mushy layer is replaced by fresher liquid from below with a greater phase transition temperature. This liquid allows further growth of ice in the mushy layer, which increases its solid fraction affecting the thermal, acoustic, electromagnetic, and mechanical properties of sea ice. Therefore, the solid fraction is an important variable of sea ice which increases rapidly once internally driven convection begins [30]. An important point is that the brine channels, which have been observed both in the laboratory [29,31] and in the field [32,33] occupy the full thickness of the mushy region.

The formation of brine channels during crystallization process has a significant impact on the structure of the mushy layer. They are responsible for the formation of another solidification scenario and generation of corrugations of the sea ice – ocean interface. The physical mechanism relies on brine flows developing in the sea ice due to Bernoulli suction by flow of ocean past the liquid – mushy layer interface. This mechanism should be particularly very important during sea ice freezing in wind-maintained coastal polynyas and in leads. Generally speaking, a true criterion of the formation of such regime is connected with the morphological instability analysis of the mushy layer crystallization with respect to small perturbations of its morphology. Such flow-induced morphological instability analysis with some model simplifications in the absence of the diffusion transport in the mush and liquid was carried out in refs. [16,17]. In the present study, we develop the morphological instability analysis of the directional crystallization with brine channels in a mushy layer and give a new instability criterion taking into account perturbations in the diffusion and solid fraction distributions for the case of nonturbulent and turbulent boundary conditions at the mush – ocean interface.

THE MATHEMATICAL MODEL

Let us consider a unidirectional crystallization process illustrated in Figure 1.

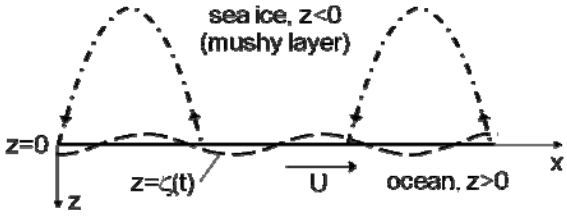

Figure 1 The geometry of the sea ice – ocean interface. The dashed line shows perturbations of the sea ice – ocean interface caused by a uniform flow in the ocean

The mushy layer (sea ice) and liquid (ocean) phases occupy regions $z<0$ and $z>0$, respectively. Convective conservation of heat and solute in the mushy layer can be expressed in differential form as:

$$\rho_m c_m(\varphi)\frac{\partial T_m}{\partial t} + \rho_l c_l \vec{u}\cdot\nabla T_m = \nabla\left[k_m(\varphi)\nabla T_m\right] + \rho_s L\frac{\partial \varphi}{\partial t} \qquad (1)$$

$$(1-\varphi)\frac{\partial C_m}{\partial t} + \vec{u}\cdot\nabla C_m = \nabla\left[D_m(\varphi)\nabla C_m\right] + (1-k_0)C_m\frac{\partial \varphi}{\partial t} \qquad (2)$$

$$T_m = T_* - mC_m \qquad (3)$$

where the terms proportional to $\partial\varphi/\partial t$ express the release of latent heat into the mush and of solute into the interstitial fluid. Condition (3) represents the liquidus equation in a linear form. The thermal properties of the mush are assumed to be volume-fraction-weighted averages of the properties of the individual phases [34]:

$$k_m(\varphi) = k_l(1-\varphi) + k_s\varphi\,,\ D_m(\varphi) = D_l(1-\varphi) \qquad (4)$$

$$\rho_m c_m(\varphi) = \rho_l c_l(1-\varphi) + \rho_s c_s\varphi$$

Expressions (4) are realistic for elongated crystals met in natural condions during seawater freezing [27].

At the mushy layer – liquid interface we have the following boundary conditions [15,35]:

$$\rho_s L\varphi_b V = k_m(\varphi_b)\vec{n}\cdot\nabla T_m - k_l\vec{n}\cdot\nabla T_l \qquad (5)$$

$$(1-k_0)C_b\varphi_b V = D_l(1-\varphi_b)\vec{n}\cdot\nabla C_m - D_l\vec{n}\cdot\nabla C_l \qquad (6)$$

where subscript 'b' designates the corresponding value at the phase transition boundary. The boundary conditions (5) and (6) hold true in the case of a laminar fluid flow in the ocean.

In the case of turbulent flow, the rate of motion of the phase transition boundary 'mushy layer – liquid' undoubtedly depends on the turbulent motion in the ocean. Therefore, let us write down the boundary conditions as follows [36-38]:

$$\rho_s L\varphi_b V = k_m(\varphi_b)\vec{n}\cdot\nabla T_m - \alpha_h\rho_l c_l u_*(T_\infty - T_b) \qquad (7)$$

$$(1-k_0)C_b\varphi_b V = D_l(1-\varphi_b)\vec{n}\cdot\nabla C_m - \alpha_s u_*(C_\infty - C_b) \qquad (8)$$

The ratio of exchange coefficients α_h/α_s depends on the molecular diffusivities for heat (κ) and salt (D_l) at that $\alpha_h/\alpha_s = (\kappa/D_l)^n$ [17] with $2/3 < n < 4/5$ [39,40] (we put $35 \le \alpha_h/\alpha_s \le 70$ after Notz et al. [36]).

The interstitial brine flows within sea ice are caused by the buoyancy forces and pressure gradients. The flushing of melt water through the ice matrix during the spring-summer season is caused by the pressure head of standing melt water on the ice surface [41]. The mechanism of buoyancy driven convection (gravity drainage) during sea ice crystallization has been discussed by Wettlaufer et al. [29,42] and Weeks [43]. The fluid mechanics of brine flows in the mushy region is fundamentally the same as that of flows within porous medium [44,45]. Therefore, let us use the simplest form of a momentum equation in the mushy layer:

$$\mu\vec{u} = \Pi(\rho_l\vec{g} - \nabla p_1) = -\Pi\nabla p \qquad (9)$$

The latter is Darcy's equation, used to describe flow in a porous medium of permeability $\Pi(\varphi)$, which is a second-rank tensor because the resistance to flow within sea ice is anisotropic and is a function of the brine fraction $1-\varphi$ and the geometry of the internal phase boundaries (for details, see, among others, ref. [46]). Generally speaking, the permeabilities to vertical and horizontal flows are different. This is caused by the anisotropic structure of sea ice such as underformed congelation ice frequently met in the Arctic Ocean (the platelets of this ice are aligned perpendicular to the sea ice – ocean interface). Therefore, the permeability to vertical flows Π_v corresponds to the direction parallel to the platelets. Then, the permeability to horizontal flows can be written as $\Pi_h = \beta^2\Pi_v$, where $0 \le \beta \le 1$ [17]. Temperature and salinity gradients in the mushy layer of sea ice cause a gradient of solid fraction leading to a fall in permeability toward the sea ice – atmosphere interface. Taking into account the latter, we model the permeability by a decaying exponential [17]:

$$\Pi_v(z) = \Pi_v(0)\exp(\gamma z) \qquad (10)$$

where γ is a mushy layer parameter. Its value can be estimated on the basis of experimental data $\gamma G^{-1} \approx 1$ K^{-1} [47].

MORPHOLOGICAL INSTABILITY

Let us consider a semi-infinite layer of sea ice ($z<0$) floating upon the ocean ($z>0$), in which there is a uniform flow U parallel to the undisturbed interface ($z=0$). Let the mushy layer – ocean interface will be perturbed by the fluid flows in the ocean. Consider a behavior of a small perturbation (corrugation) to the equilibrium sea ice – ocean interface $z=0$ in the form of $z=\zeta(x,t)=\hat{\zeta}\exp(i\alpha x+\sigma t)$. In the case of irrotational flow in the ocean $\vec{u}=\nabla\Phi$, where, from continuity, the velocity potential satisfies $\nabla^2\Phi=0$. Further, let us consider the following approximation: the sea ice is practically impermeable to the external flow because the flow of brine in the mushy layer is much slower than the flow in the ocean, i.e. $\vec{n}\cdot\nabla\Phi=0$ on $z=\zeta$. In this case, the velocity potential is:

$$\Phi = U(x - i\zeta\exp(-\alpha z)) \qquad (11)$$

Substituting Φ from (11) into the linearized Bernoulli equation, we get the pressure at the interface:

$$p(x,t) = -\rho_l\alpha U^2\zeta(x,t) \qquad (12)$$

Now, combining equations (9), (10) and continuity of brine flow $\nabla\cdot\vec{u}=0$, we find an equation determining the pressure in the mushy layer:

$$\beta^2\frac{\partial^2 p}{\partial x^2} + \gamma\frac{\partial p}{\partial z} + \frac{\partial^2 p}{\partial z^2} = 0$$

Its solution is given by:

$$p(x,z,t) = -\rho_l\alpha U^2\zeta(x,t)\exp(qz),\ q = \frac{\sqrt{\gamma^2+4\alpha^2\beta^2}}{2} - \frac{\gamma}{2} \qquad (13)$$

Note, that expression (13) goes over into expresiion (12) at the phase transition interface.

As a rule, the temperature field in the mushy layer and solid phase can be regarded as a linear function of the spatial coordinate [26,48-50]. This is due to the fact that the temperature conductivities are several orders of magnitude higher than the corresponding solute diffusivities so that the concentration relaxation time exceeds greatly the temperature one. Then, we have the following perturbed temperature distribution $T(x,z,t)=T_b+Gz+\hat{\theta}(z)\exp(i\alpha x+\sigma t)$. Now, the perturbed salinity field is completely determined by expression (3). The amplitude of temperature perturbations can be found by means of equations (1)-(3) and expressions (4) and (13). To do this let us present the solid fraction in the form of the unperturbed contribution and perturbations as $\varphi(x,z,t)=\varphi_0+\hat{\Phi}(z)\exp(i\alpha x+\sigma t)$. Further, we use the quasi-stationary approximation $\partial/\partial t\to 0$, which implies that the sea

ice freezing (melting) is sufficiently slow process, and the temperature, salinity and solid fraction fields evolve to the steady-state profiles. Numerical calculations show that the quasi-stationary approximation gives accurate stability curves [16].

Eliminating the salinity field from equation (2) by means of expression (3), we come to two nonlinear equations for perturbations from the governing set (1) and (2). Further, eliminaiting from these equations summands proportional to φ_0 and $\hat{\Phi}$, we arrive at the differential equation for the determination of temperature amplitude:

$$\frac{d^2\hat{\theta}}{dz^2} - \alpha^2\hat{\theta} = A\exp[(\gamma+q)z] \qquad (14)$$

$$A = \left(1 + \frac{\kappa(K-1)}{KD_l}\right)\frac{\Pi_v(0)\alpha U^2 qG\hat{\zeta}}{\kappa\nu}$$

$$\kappa = \frac{k_s}{\rho_l c_l},\ K = \frac{k_s}{k_l},\ \nu = \frac{\mu}{\rho_l}$$

where, for the sake of simplicity, we have ignored the acceleration due to gravity. Note, that $\hat{\theta}$ is bounded as $z \to -\infty$ and $\hat{\theta}(0) = -G\hat{\zeta}$. Taking into account these boundary conditions, we find the solution of equation (14):

$$\hat{\theta}(z) = -G\hat{\zeta}\exp(\alpha z) + \frac{A[\exp((q+\gamma)z) - \exp(\alpha z)]}{(q+\gamma)^2 - \alpha^2} \qquad (15)$$

for the anisotropic and heterogeneous permeability ($\beta \neq 1$ and $\gamma \neq 0$), and:

$$\hat{\theta}(z) = -G\hat{\zeta}\exp(\alpha z) + \frac{Az}{2\alpha}\exp(\alpha z) \qquad (16)$$

for the isotropic and homogeneous permeability ($\beta = 1$ and $\gamma = 0$).

Now, eliminating φ_b from expressions (5) and (6), and keeping in mind the boundary condition of marginal equilibrium [15]:

$$\left(\frac{\partial T_l}{\partial z}\right) = -m\left(\frac{\partial C_l}{\partial z}\right)$$

we obtain the following relation at the phase transition interface:

$$\rho_s LV = k_s\frac{\partial T_m}{\partial z} + \frac{(1-k_0)k_l(T_b - T_*)V}{D_l} \qquad (17)$$

Expanding (17) in a series in perturbations in the neighborhood of a point $z = 0$ and taking into account only linear terms, after substitution of expressions (15) and (16), we get the growth rate of perturbations in the classical non-turbulent case:

$$\sigma = \alpha V_1\left(\frac{A_*}{q+\gamma+\alpha} - 1\right) - \frac{(1-k_0)V_1^2}{KD_l},\ \beta \neq 1,\ \gamma \neq 0 \qquad (18)$$

$$\sigma = \alpha V_1\left(\frac{A_*}{2\alpha} - 1\right) - \frac{(1-k_0)V_1^2}{KD_l},\ \beta = 1,\ \gamma = 0$$

$$A_* = \frac{A}{\alpha G\hat{\zeta}},\ V_1 = \frac{k_s GD_l}{\rho_s LD_l - (1-k_0)k_l(T_b - T_*)}$$

Now, eleminating φ_b from the boundary conditions (7) and (8), we have the following expression at the mushy layer – ocean interface:

$$\left[\rho_s LV - (k_s - k_l)\frac{\partial T_m}{\partial z}\right]\left[D_l\frac{\partial T_m}{\partial z} + \alpha_s u_*(mC_\infty - T_* + T_b)\right] = \qquad (19)$$

$$= \left[k_l\frac{\partial T_m}{\partial z} - \alpha_h\rho_l c_l u_*(T_\infty - T_b)\right]\left[D_l\frac{\partial T_m}{\partial z} - (1-k_0)(T_* - T_b)V\right]$$

As before, expanding (19) in series, we come to the growth rate of perturbations in the case of turbulent fluxes in the ocean:

$$\sigma = \frac{P(D_l a_1 + k_l a_2 - D_l a_3 + a_4) - G(a_1(1-k_0)V_2 + a_2\rho_l c_l\alpha_h u_* - a_3\alpha_s u_*)}{a_5}$$

$$P = \frac{d\hat{\theta}/dz}{\hat{\zeta}},\ V_2 = G\frac{a_1 D_l + a_4}{a_5} \qquad (20)$$

$$a_1 = k_l G - \rho_l c_l\alpha_h u_*(T_\infty - T_b),\ a_2 = D_l G - (T_* - T_b)(1-k_0)V_2$$

$$a_3 = \rho_s LV_2 - (k_s - k_l)G,\ a_5 = \frac{\rho_s La_4}{k_s - k_l} + (T_* - T_b)(1-k_0)a_1$$

$$a_4 = (k_s - k_l)[D_l G + \alpha_s u_*(mC_\infty - T_* + T_b)]$$

Substitution $d\hat{\theta}/dz$ at $z = 0$ from (15) or (16) in (20) gives the growth rate for the anisotropic and heterogeneous or isotropic and homogeneous permeability. The case of negative values of σ corresponds to morphological stability of the process, whereas the opposite case of positive σ describes convective instability caused by fluid flows in the mushy layer.

DISCUSSION

Expressions (18) and (20) are the central result of our theory. Figures 2 and 3 demonstrate that the non-turbulent theory under consideration taking into account perturbations of the salinity and bulk fraction distributions essentially differs from the formely known criterion of the "purely" thermal problem deduced in ref. [17].

The neutral stability curves (solid and chain-dotted lines) give different stability domains: the present theory shows that the instability domain becomes widely for each of the curves. From the physical point of view this is due to the fact that the impurity displacement by the growing solid material increases brine salinity and decreases phase transition temperature, and in its turn increases structural and phase inhomogeneitis in the mushy layer and leads to its instability.

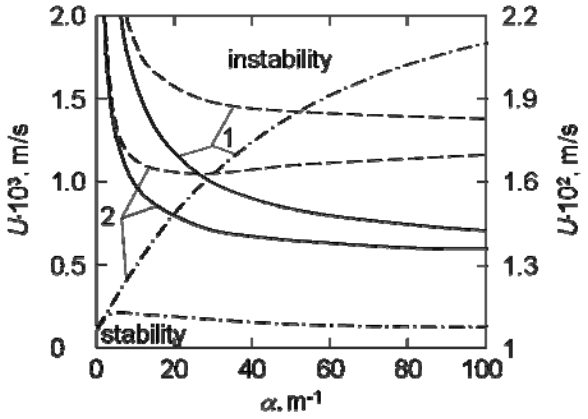

Figure 2 Neutral stability curves ($\sigma = 0$) calculated for non-turbulent (solid lines, scale of values on the left, expressions (18)) and turbulent (dashed lines, scale on the left, expressions (20)) conditions. Chain-dotted lines demonstrate approximate theory developed in ref. [17] (scale on the right); $\beta = 0.1$ - (1) and $\beta = 1$ - (2), $\gamma = 10$ m^{-1}. System parameters are $D_l = 10^{-9}$ m^2/s, $\nu = 1.07\cdot10^{-6}$ m^2/s, $\Pi = 10^{-8}$ m^2, $k_s = 2.22$ J/(m·s·K), $k_l = 0.59$ J/(m·s·K), $\rho_l = 10^3$ kg/m^3, $\rho_s = 920$ kg/m^3, J/(kg·K), $G = 50$ K/m, $m = 5.3\cdot10^{-2}$ K/psu, $L = 3.35\cdot10^5$ J/kg, $u_* = 5\cdot10^{-4}$ m/s, $\alpha_h = 0.0095$, $\alpha_s = \alpha_h/35$, $T_\infty = 274$ K, $S_\infty = 35$ psu, $T_b = 271$ K, $T_* = 273$ K, $k_0 = 0$

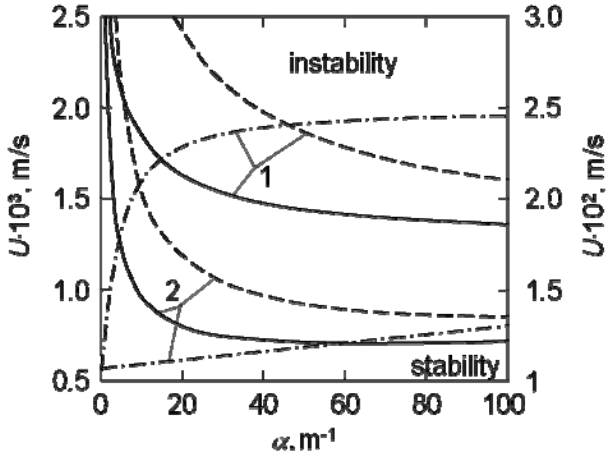

Figure 3 Neutral stability curves ($\sigma = 0$) calculated for non-turbulent (solid lines, scale on the left, expressions (18)) and turbulent (dashed lines, scale on the left, expressions (20)) conditions. Chain-dotted lines demonstrate approximate theory developed in ref. [17] (scale on the right); $\gamma = 1$ m^{-1} - (1) and $\gamma = 100$ m^{-1} - (2), $\beta = 0.1$. Regions of morphological instability and stability lie above and under each curve, respectively

Figure 2 illustrates that decreasing the coefficient of permeability β gives more wide stability region for a fixed value of wavenumber α due to weakening of the convective transfer in the phase transition domain. At the same time an increase in the coefficient of inhomogeneity γ results in a build up of instability region because of increased heat and mass transfer (Figure 3).

Let us emphasize several features of the instability criterion (18). The enhancement of viscocity ν decreas es parameter A_* and moves the system into stability region. The opposite case occurs when the fluid velocity U increases. If this velocity is fixed, an increase of the wave number α leads the process into instability whereas the criterion obtained in ref. [17] gives the opposite tendency (solid and chain-dotted lines in Figures 2 and 3). From the physical point of view this conclusion can be explained as follows: perturbations with a small wave length (inversly proportional to α) form more easily different inhomogeneities. It is reasonable to expect that perturbations form inhomogeneities whose length is of the order of a characteristic length of perturbations (to form a smaller size of inhomogeneity we need to overcome a smaller energy barrier).

Let us calculate the growth rate of corrugations responsible for the turbulent flows near the phase transition interface. While estimating σ in (18) as $10^{-5} - 10^{-4}$ s^{-1}, we see that a 1 cm corrugation will grow to several times in size for several hours. A detailed description of this problem can be performed within the framework of the nonlinear stability theory. Such instability analysis devoted to the evolution of oscillatory instability near the neutral stability curve can be carried out in the spirit of works [51,52].

Comparing corresponding solid and dashed lines in Figures 2 and 3 it is easily seen that the stability region becomes wider in the turbulent model at fixed velocity U .The same behavior occurs with increasing the friction velocity and turbulent coefficient for heat (compare corresponding curves in Figure 4). This is due to the fact that the turbulent boundary conditions involve taking account of friction forces at the mushy layer – ocean interface playing the role of a stabilizing factor.

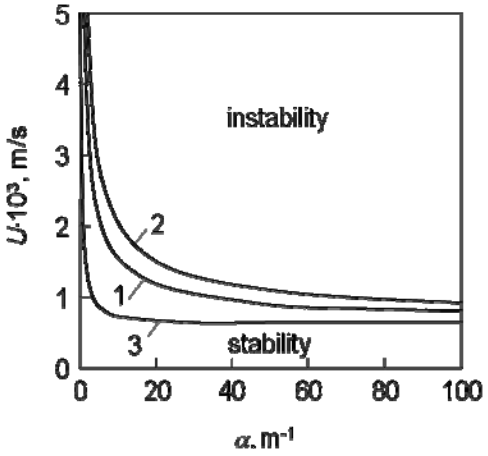

Figure 4 Neutral stability curves ($\sigma = 0$) calculated for turbulent conditions: $u_* = 5\cdot10^{-4}$ m/s, $\alpha_h = 0.0095$ - (1), $u_* = 10^{-3}$ m/s, $\alpha_h = 0.0095$ - (2), $u_* = 5\cdot10^{-4}$ m/s, $\alpha_h = 0.0035$ - (3). Regions of morphological instability and stability lie above and under each curve, respectively

CONCLUSION

Since the two-phase region appears as the result of the concentration supercooling and development of morphological instability of the plane front described in a classic study [53], only the dynamic instability consisting of oscillations of the two-phase region as a whole with a zero wave number is possible in the absence of convection. The stability of the phase transition region with respect to such oscillations, which are most dangerous (growing), was investigated previously in [54]. It is shown in Figure 5 that the convective instability extends the region of dynamic instability (the solid line extends the region of dynamic instability I to the region of convective instability I and II determined by the solid curve). In this case, as the velocity of the convective flow increases, the instability region substantially broadens (solid and dash-and-dot lines in Figure 5). In actual processes, the phase transition almost always occurs in the extended region and in the presence of convective flows of the liquid.

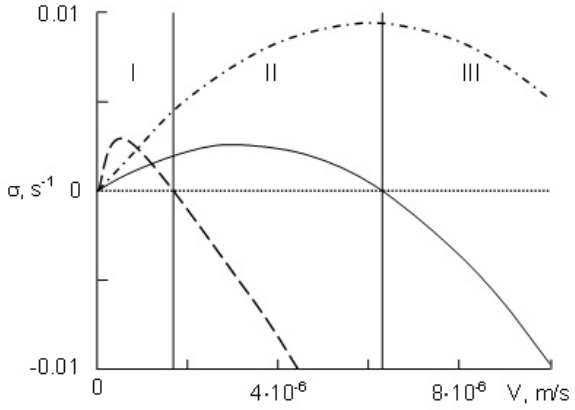

Figure 5 Dependence of the instability parameter on the crystallization rate. The solid and dash-and-dot lines are constructed by formula (18) at $\alpha = 10\ m^{-1}$, $\beta = 0.5$, $\gamma = 10\ m^{-1}$, $U = 8 \times 10^{-3}$ m/s, and $U = 11 \times 10^{-3}$ m/s, respectively. The dashed line is constructed by formula (38) from [54] (the scale σ is increased by a factor of 1000). The points of intersection of the curves with the horizontal line show the transition through the curve of neutral stability. Vertical lines border three regions of the process: region I corresponds to the dynamic and convective instability, region II corresponds to the dynamic stability and convective instability, and region III is the dynamic and convective stability

In conclusion, let us denote that the instability criteria (18) and (20) determine different regimes of the crystallization process with a mushy layer in the presence ($\sigma > 0$) or absence ($\sigma < 0$) of brine channels leading to the formation of a corrugated sea ice – ocean interface, redistributions of the salinity and solid fraction in the mushy layer and changes in the heat flux between the ocean and the atmosphere.

This work was made possible in part by the Federal Target Program "Scientific and Academic – Teaching Staff of Innovative Russia" in 2009 – 2013 and Russian Foundation for Basic Research (project No 10-01-96045 Ural).

REFERENCES

[1] Rubinshtein L.I., The Stefan Problem, AMS, Providence, 1971.

[2] Meirmanov A.M., The Stefan Problem, De Gruyter, Berlin, 1992.

[3] Ivantsov G.P., Diffusive supercooling in binary alloy solidification, *Dokl. Akad. Nauk SSSR*, Vol. 81, 1951, pp. 179–182 (in Russian).

[4] Sekerka R.F., Morphological stability, *in: P. Hartman (Ed.), Crystal Growth: An Introduction*, North-Holland, 1973, pp. 403–442.

[5] Langer J.S., Instabilities and pattern formation in crystal growth, *Rev. Mod. Phys.*, Vol. 52, 1980, pp. 1–28.

[6] Copley S.M., Giamei A.F., Johnson S.M., and Hornbecker M.F., The origin of freckles in unidirectionally solidified castings, *Metall. Trans.*, Vol. 1, 1970, pp. 2193–2204.

[7] Chen C.F., and Turner J.S., Crystallization in double-diffusive system, *J. Geophys. Res.*, Vol. 85, 1980, pp. 2573–2593.

[8] Worster M.G., Huppert H.E., and Sparks R.S., Convection and crystallization in magma cooled from above, *Earth Planet. Sci. Lett.*, Vol. 101, 1990, pp. 78–89.

[9] Loper D.E., Structure of the inner core boundary, *Geophys. Astrophys. Fluid Dyn.*, Vol. 25, 1983, pp. 139–155.

[10] Hills R.N., Loper D.E., and Roberts P.H., A thermodynamically consistent model of a mushy zone, *Quart. J. Appl. Math.*, Vol. 36, 1983, pp. 505–539.

[11] Fowler A.C., The formation of freckles in binary alloys, *IMA J. Appl. Math.*, Vol. 35, 1985, pp. 159–174.

[12] Alexandrov D.V., Theory of solidification with a quasi-equilibrium two-phase zone, *Phys.-Dokl.*, Vol. 45, 2000, pp. 569–573.

[13] Alexandrov D.V., Solidification with a quasiequilibrium mushy region: exact analytical solution of nonlinear model, *J. Cryst. Growth*, Vol. 222, 2001, pp. 816–821.

[14] Alexandrov D.V., Solidification with a quasiequilibrium two-phase zone, *Acta Mater.*, Vol. 49, 2001, pp. 759–764.

[15] Worster M.G., Solidification of an alloy from a cooled boundary, *J. Fluid Mech.*, Vol. 167, 1986, pp. 481–501.

[16] Feltham D.L., and Worster M.G., Flow-induced morphological instability of a mushy layer, *J. Fluid Mech.*, Vol. 391, 1999, pp. 337–357.

[17] Feltham D.L., Worster M.G., and Wettlaufer J.S., The influence of ocean flow on newly forming sea ice, *J. Geophys. Res.*, Vol. 107, 2002, Article No. 3009.

[18] Hellawell A., Sarazin J.R., and Steube R.S., Channel convection in partly solidified systems, *Philos. Trans. Roy. Soc. Lond.*, Vol. A345, 1993, pp. 507–544.

[19] Eide L.I., and Martin S., The formation of brine drainage features in young sea ice, *J. Glaciol.*, Vol. 14, 1975, pp. 137–154.

[20] Tait S., and Jaupart C., Compositional convection in a reactive crystalline mush and melt differentiation, *J. Geophys. Res.*, Vol. 97, 1992, pp. 6735–6756.

[21] Fearn D.R., Loper D.E., and Roberts P.H., Structure of the Earth's inner core, *Nature*, Vol. 292, 1981, pp. 232–233.

[22] Bergman M.I., and Fearn D.R., Chimneys on the Earth's inner-outer core boundary, *Geophys. Res. Lett.*, Vol. 21, 1994, pp. 477–480.
[23] Aagaard K., and Carmack E., The arctic ocean and climate: a perspective, *in: O.M. Johannessen, R.D. Muench, J.E. Overland (Eds.), The Polar Regions and their Role in Shaping the Global Environment, Geophys. Monogr. Ser.*, Vol. 85, AGU, 1994, pp. 5–20.
[24] Rahmstorf S., Bifurcations of the Atlantic thermohaline circulation in response to changes in the hydrological cycle, *Nature*, Vol. 378, 1995, pp. 145–149.
[25] Morison J.H. et al., The Lead experiment, *EOS Trans. AGU*, Vol. 74, 1993, pp. 393–397.
[26] Wettlaufer J.S., Worster M.G., and Huppert H.E., Solidification of leads: theory, experiment and field observations, *J. Geophys. Res.*, Vol. 105, 2000, pp. 1123–1134.
[27] Perovich D.K., and Richter-Menge J.A., Ice growth and solar heating in springtime leads, *J. Geophys. Res.*, Vol. 105, 2000, pp. 6541–6548.
[28] Alexandrova I.V., Alexandrov D.V., Aseev D.L., and Bulitcheva S.V., Mushy layer formation during solidification of binary alloys from a cooled wall: the role of boundary conditions, *Acta Phys. Pol. A*, Vol. 115, 2009, pp. 791–794.
[29] Wettlaufer J.S., Worster M.G., and Huppert H.E., The phase evolution of young sea ice, *Geophys. Res. Lett.*, Vol. 24, 1997, pp. 1251–1254.
[30] Worster M.G., and Wettlaufer J.S., Natural convection, solute trapping, and channel formation during solidification of saltwater, *J. Phys. Chem. B*, Vol. 101, 1997, pp. 6132–6136.
[31] Bennington K.O., Some crystal growth features of sea ice, *J. Glaciol.*, Vol. 4, 1963, pp. 669–688.
[32] Lake R.A., and Lewis E.L., Salt rejection by sea ice during growth, *J. Geophys. Res.*, Vol. 75, 1970, pp. 583–597.
[33] Perovich D.K., and Richter-Menge J.A., Loss of sea ice in the Arctic, *Annu. Rev. Mar. Sci.*, Vol. 1, 2009, pp. 417–441.
[34] Batchelor G.K., Transport properties of two-phase materials with random structure, *Ann. Rev. Fluid Mech.*, Vol. 6, 1974, pp. 227–255.
[35] Worster M.G., Natural convection in a mushy layer, *J. Fluid Mech.*, Vol. 224, 1991, pp. 335–359.
[36] Notz D., McPhee M.G., Worster M.G., Maykut G.A., Schlunzen K.H., and Eicken H., Impact of underwater-ice evolution on Arctic summer sea ice, *J. Geophys. Res.*, Vol. 108 (C7), 2003, pp. 3223.
[37] McPhee M.G., The upper ocean, *in: N. Untersteiner (Ed.), The Geophysics of Sea Ice*, Plenum, New York, 1986, pp. 133–141.
[38] McPhee M.G., Maykut G.A., and Morison J.H., Dynamics and thermodynamics of the ice/upper ocean system in the marginal ice zone of the Greenland sea, *J. Geophys. Res.*, Vol. 92 (C7), 1987, pp. 7017–7031.
[39] Owen P.R., and Thomson W.R., Heat transfer across rough surfaces, *J. Fluid Mech.*, Vol. 15, 1963, pp. 321–334.
[40] Yaglom A.M., and Kader B.A., Heat and mass transfer between a rough wall and turbulent flow at high Reynolds and Peclet numbers, *J. Fluid Mech.*, Vol. 62, 1974, pp. 601–623.
[41] Untersteiner N., Natural desalinisation and equilibrium salinity profile of sea ice, *J. Geophys. Res.*, Vol. 73, 1968, pp. 1251–1257.
[42] Wettlaufer J.S., Worster M.G., and Huppert H.E., Natural convection during solidification of an alloy from above with application to the evolution of sea ice, *J. Fluid Mech.*, Vol. 344, 1997, pp. 291–316.
[43] Weeks W.F., Growth conditions and the structure and properties of sea ice, *in: M. Lepparanta (Ed.), Physics of Ice-Covered Seas*, Univ. of Helsinki Press, 1998, pp. 24–104.
[44] Bear J., Dynamics of Fluids in Porous Media, Elsevier Science, New York, 1972.
[45] Phillips O., Flow and Reactions in Permeable Rocks, Cambridge University Press, New York, 1991.
[46] Katz R.F., and Worster M.G., Simulation of directional solidification, thermochemical convection, and chimney formation in a Hele-Shaw cell, *J. Comput. Phys.*, Vol. 227, 2008, pp. 9823–9840.
[47] Ono N., and Kasai T., Surface layer salinity of young sea ice, *Ann. Glaciol.*, Vol. 6, 1980, pp. 298–299.
[48] Alexandrov D.V., Malygin A.P., and Alexandrova I.V., Solidification of leads: approximate solutions of non-linear problem, *Ann. Glaciol.*, Vol. 44, 2006, pp. 118–122.
[49] Alexandrov D.V., and Malygin A.P., Analytical description of seawater crystallization in ice fissures and their influence on heat exchange between the ocean and the atmosphere, *Dokl. Earth Sci.*, Vol. 411A, 2006, pp. 1407–1411.
[50] Martin S., and Kauffman P., The evolution of under-ice melt ponds, or double diffusion at the freezing point, *J. Fluid Mech.*, Vol. 64, 1974, pp. 507–527.
[51] Wollkind D.J., and Segel L.A., A nonlinear stability analysis of the freezing of a dilute binary alloy, *Philos. Trans. Roy. Soc. A*, Vol. 268, 1970, pp. 351–380.
[52] Stuart J.T., Nonlinear stability theory, *Ann. Rev. Fluid Mech.*, Vol. 3, 1971, pp. 347–370.
[53] Mullins W.W., and Sekereka R.F., Stability of a planar interface during solidification of a dilute binary alloy, *J. Appl. Phys.*, Vol. 35, 1964, pp. 444–451.
[54] Alexandrov D.V., and Ivanov A.O., Dynamic stability analysis of the solidification of binary melts in the presence of a mushy region: changeover of instability, *J. Cryst. Growth*, Vol. 210, 2000, pp. 797–810.